

Effects of Immersion Time and Temperature on the Corrosion of API 5L Grade X-65 Steel in 1.0 M H₂SO₄ Pickling Solution

Asiful H. Seikh¹ and El-Sayed M. Sherif^{1,2,*}

¹College of Engineering, King Saud University, P.O. Box - 800, Riyadh 11421, Saudi Arabia

²Electrochemistry and Corrosion Laboratory, Department of Physical Chemistry, National Research Centre (NRC), Dokki, 12622 Cairo, Egypt

*E-mail: esherif@ksu.edu.sa; emsherif@gmail.com

Received: 27 September 2014 / Accepted: 11 November 2014 / Published: 2 December 2014

The aim of the present work was to report the effect of increasing the immersion time and the solution temperature on the electrochemical corrosion behavior of API 5L grade X-65 pipeline steel in 1.0 M H₂SO₄ pickling solutions using different experimental measurements. The potentiodynamic polarization results showed that increasing the immersion time from 10 min to 60 min and further to 24 h for the steel in the sulfuric acid solution before measurements increased the anodic and cathodic currents and corrosion current density (j_{Corr}) and decreased the polarization resistance (R_p). Electrochemical impedance spectroscopy (EIS) measurements confirmed the polarization data that the increase of immersion time decreases the solution and polarization resistances. Both polarization and EIS data also revealed that increasing the solution temperature in the range from 20 °C to 60 °C highly increased the corrosion of the X-65 steel due to the faster and contentious dissolution of the surface with temperature. Results collectively were consistent with others and proved clearly that the corrosion of the investigated steel in the 1.0 M H₂SO₄ solution increases with elongating the immersion time as well as increasing the solution temperature.

Keywords: corrosion; X-65 steel; acidic pickling solutions; EIS; polarization

1. INTRODUCTION

API 5L grade X-65 is considered as a high-strength low alloy (HSLA) steel that has wide range of applications in chemical processing, construction and metal processing equipment, oil / gas storage tanks, marine applications and transportation pipelines due to its high strength and toughness, good weldability and formability [1,2]. The structures of these steels, i.e., pipe lines, off-shore rigs, agitators, pumps, and tanks, are exposed to severe conditions of corrosion due to the aggressive chemical

solutions [3-5] loaded with impurities (chlorides, sulfates etc.) contained in the mineral or introduced into the wash water with other thermal (temperature) and mechanical (abrasion) constraints [6-8].

The corrosion of steel in acidic solutions is an industrial concern that has received a considerable amount of attention [9]. Corrosion is a serious problem in steel pipelines because replacing, repairing and maintaining them can be extremely expensive and time-consuming [10–13]. The water content associated with the oil production process has been found to be a significant factor in the internal corrosion of steel pipelines because the water contains many corrosive agents such as carbon dioxide, hydrogen sulphides, organic acids, and salts [14–19]. Kwok et al. [20] and Ma and Wang [21] studies that pipeline failures usually occur not as a result of uniform corrosion but in the form of localized attack, generally as pitting or galvanic corrosion of welds. These forms of attack can cause pipeline degradation that can lead to spillage of products resulting in environmental catastrophes.

The service life of pipeline steels is affected not only by the fluid or gas which they transfer, but also by the environmental conditions under which they operate. One of the main reasons for the degradation in mechanical properties of steels is the exposure to environment. For example, on exposure to a sour gas environment, the steel surface corrodes and produces hydrogen at the surface. This hydrogen can be absorbed in the steel and can then start diffusing to regions of stress concentration, impairing ductility and promoting brittle behavior (hydrogen embrittlement). The diffusion of hydrogen in steels is affected by the microstructure of the steel: the phase or phases present, grain boundaries, grain shapes, vacancies and dislocations, interfaces with nonmetallic inclusions, precipitate particles and voids [22-24].

The aim of the present work was to investigate the corrosion behavior of API 5L X-65 steel grade after different periods of immersion, namely 10 min, 60 min, and 24, at different temperatures in 1.0 M H₂SO₄ acidic pickling solution. The study was carried out using linear polarization and electrochemical impedance spectroscopy techniques. The microstructure of the X-65 pipeline steel has also been performed to provide a foundation for the understanding of the corrosion mechanism.

2. EXPERIMENTAL DETAILS

2.1. Materials and solution preparation

The API X-65 5L pipeline steel grade was cut into coupons of dimensions 10 × 10 × 5 mm from hot-rolled plate of 15mm thickness. The typical chemical compositions of the elements present in the steel in wt. % are listed in Table 1. The coupons were degreased with acetone, air dried and embedded into two-component epoxy resin and mounted in a glass holder. A copper wire was soldered to the rear side of the coupon as an electrical connection. Prior to each experimental run, the exposed surface of the electrode (of area 100 mm²) was wet polished with silicon carbide abrasive papers up to 1000 grit, rinsed with ethanol and finally dried in air. The acidic test, 1.0 M H₂SO₄ solution was prepared from analytical grade reagent and distilled water. While the electrolyte solutions were in

equilibrium with the atmosphere, all experiments were carried out under thermostatic conditions 25°C ($\pm 0.1^\circ\text{C}$).

Table 1. Chemical compositions in wt. % of spiral welded API X-65 5L pipeline steel sample.

Element	C	Si	Mn	P	S	Al	Ti	Cu	Cr	Nb + V	Fe
Wt. %	0.08	0.25	1.5	0.01	0.002	0.05	0.02	0.003	0.016	< 0.12	Balance

2.2. Optical microscopy

One of the surfaces of the spiral welded API X-65 5L pipeline steel was mechanically ground on the silicon carbide abrasive papers sequentially on 60, 120, 240, 320, 400, 600, and 1000 grit silicon carbide papers and polished on a Sylvet cloth using coarse and fine Geosyn- Grade I slurry of Al_2O_3 . This surface was cleaned, washed by water, alcohol, dried in air and then etched in 2% Nital solution (2% HNO_3 in ethanol). The etched specimen was observed by XJL-03 model metallographic microscope and the microstructure was taken with the help of a Camera fitted with the microscope.

2.3. Electrochemical Measurements

Electrochemical experiments were performed in a conventional three-electrode cell accommodates for 200 mL solution. An Ag/AgCl and a platinum foil were used as the reference and counter electrode, respectively. All potentials quoted in this paper were referred to the Ag/AgCl. Whereas, the polished API 5L X-65 steel rod with its total surface area of 1 cm^2 was used as the working electrode. All electrochemical experiments were carried out using an Autolab Potentiostat (PGSTAT20, computer controlled) operated by the general purpose electrochemical software (GPES) version 4.9. The free corrosion potential (versus Ag/AgCl) was followed after immersing the working electrode in the test solution until the potential stabilized within $\pm 1\text{ mV} / \text{min}$. This was followed by electrochemical impedance spectroscopy (EIS) test and the data were recorded at the corrosion potential (E_{Corr}). The frequency was scanned from 100 KHz to 100 mHz, with an ac wave of $\pm 5\text{ mV}$ peak-to-peak overlaid on a dc bias potential. The best equivalent circuit of Nyquist plots was calculated by fit and simulation method. The potentiodynamic polarization curves were obtained by scanning the potential in the forward direction from -0.1 to 0.1 V against Ag/AgCl at a scan rate of 1 mV/s .

All the electrochemical experiments were recorded after immersion of the electrode in the test solution at a temperature of $(25 \pm 1)^\circ\text{C}$. Fresh solution and fresh specimens were used in each weep and three measurements were performed to ensure the reliability and reproducibility of the data.

3. RESULTS

3.1. Metallographic investigations

Fig. 1 shows the microstructure of the API X-65 5L pipeline steel, which is composed of polygonal ferrite (PF) and quasi polygonal ferrite (QPF) matrix (α) and pearlite. Precipitates of carbides at ferrite grain boundaries, and some small precipitates inside the ferrite grains in which the polygonal ferrite is the dominant phase leading to enhanced weldability and satisfactory strength. The PF grains have equiaxed, smooth and continuous boundaries, and the QPF grains have irregular and jagged boundaries, containing subboundaries.

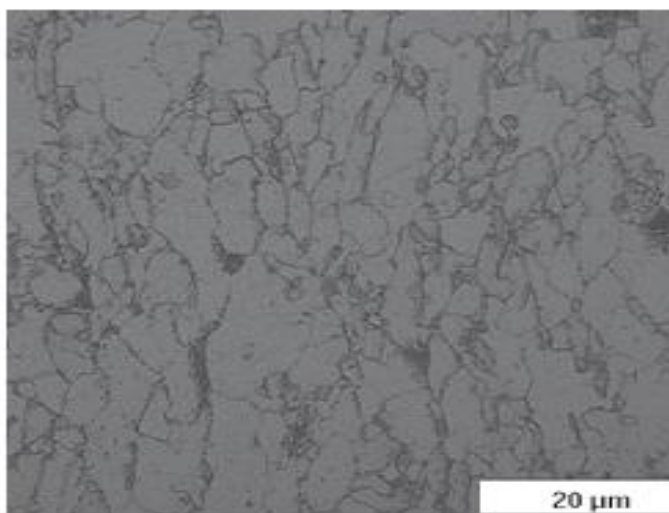


Figure 1. Microstructure of the API X-65 5L pipeline steel under investigation.

3.2. Potentiodynamic polarization measurements

In order to study the effect of immersion time on the corrosion behavior of the API X-65 5L pipeline steel, the polarization curves were obtained after 10 min, 60 min and 24 h of immersion in 1.0 M H_2SO_4 solution at room temperature as shown in Fig. 2. The polarization parameters obtained from the curves shown in Fig. 2 are listed in Table 2. These parameters include the values of corrosion current densities (j_{Corr}), corrosion potential (E_{Corr}), cathodic (β_c) and anodic (β_a) Tafel slopes, and polarization resistance (R_p). The values of (β_c), (β_a), j_{Corr} , E_{Corr} , and R_p were determined according to our previous study [25]. It is clearly seen from Fig. 2 and Table 2 that increasing the immersion time from 10 min to 24 h shifts the E_{Corr} toward the less negative values, increases the corrosion of the steel through increasing the values of j_{Corr} and decreasing the corresponding R_p values.

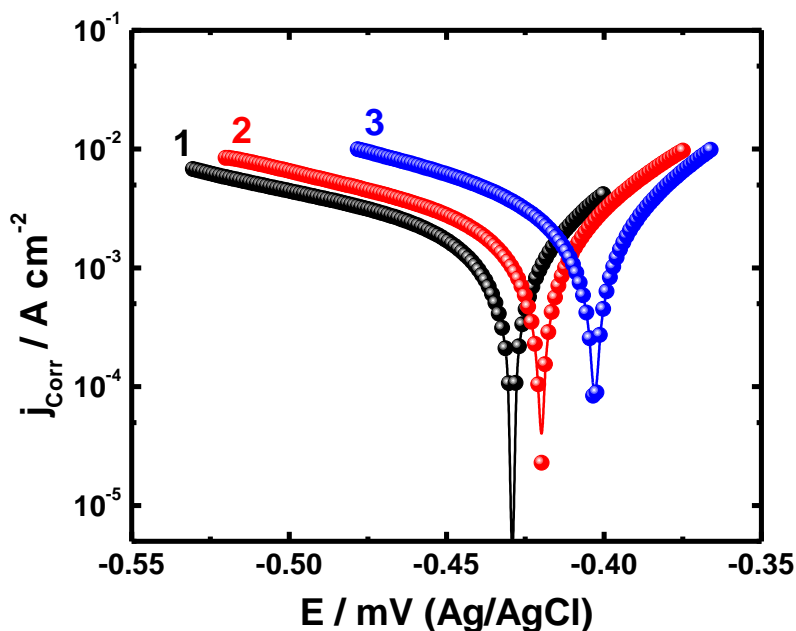


Figure 2. Potentiodynamic polarization curves obtained for X-65 5L pipeline steel samples after (1) 10 min, (2) 60 min and (3) 24 h immersion in 1.0 M H₂SO₄ solutions at room temperature.

Table 2. Potentiodynamic polarization parameters of the API X-65 steel after 10 min, 60 min and 24 h immersion in 1.0 M H₂SO₄ at room temperature.

	Parameter				
time	$\beta_a / \text{mVdec}^{-1}$	$\beta_c / \text{mV/dec}^{-1}$	$E_{\text{Corr}} / \text{mV}$	$j_{\text{Corr}} / \mu\text{A cm}^{-2}$	$R_p \Omega \text{cm}^2$
10 min	28.76	21.65	-429	384.7	13.95
60 min	40.78	27.53	-420	635.6	11.23
24 h	28.48	25.2	-403	739.5	7.85

In order to report the effect of increasing temperature on the corrosion behavior of the API X-65 5L pipeline steel, we carried out polarization measurements at 20, 30, 40, 50, and 60 °C and the curves are shown respectively in Fig. 3. The corresponding corrosion parameters obtained for the steel from Fig. 3 are recorded in Table 3. The measurements indicated that the increase of temperature increases the corrosion of the X-65 steel in 1.0 M H₂SO₄ via increasing the values of j_{Corr} and decreasing the values of R_p .

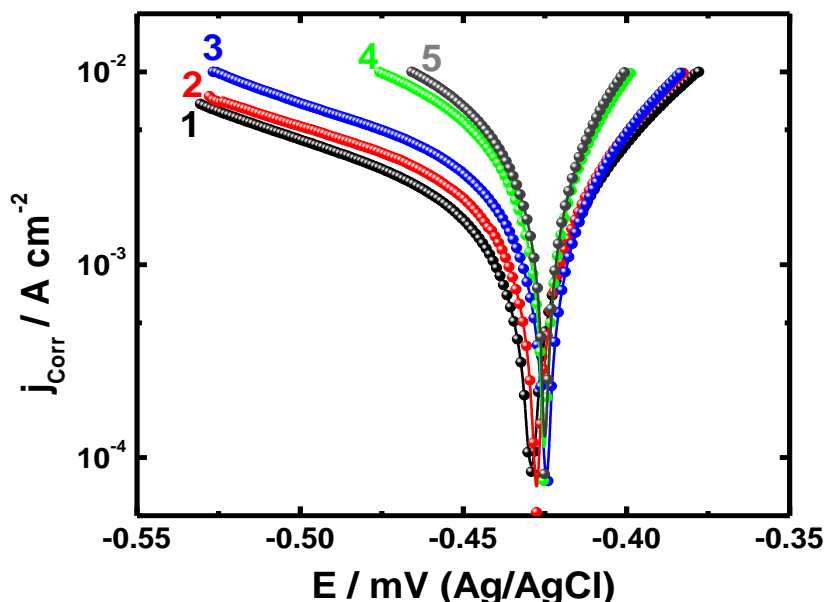


Figure 3. Potentiodynamic polarization curves obtained for the API X-65 steel after 30 min immersion in 1.0 M H₂SO₄ solutions (1) 20 °C, (2) 30 °C, (3) 40 °C, (4) 50 °C and (5) 60 °C, respectively.

Table 3. Potentiodynamic polarization parameters obtained for the API X-65 pipeline steel after 30 min immersion in 1.0 M H₂SO₄ at different temperature.

Temperature	Corrosion parameters				
	$\beta_a / \text{mVdec}^{-1}$	$\beta_c / \text{mVdec}^{-1}$	$E_{\text{Corr}} / \text{mV}$	$j_{\text{Corr}} / \mu\text{A cm}^{-2}$	$R_p \Omega \text{ cm}^2$
20 °C	28.76	21.65	-429	384.7	13.95
30 °C	33.17	24.89	-427	551.8	11.19
40 °C	38.45	26.71	-423	796.4	8.59
50 °C	22.68	17.64	-425	972.2	4.43
60 °C	24.74	17.95	-424	1052.2	4.29

3.3. Electrochemical impedance spectroscopy (EIS) measurements

EIS is a powerful technique that has been widely employed to understand the mechanism of corrosion and passivation phenomena for different metals and alloys in a variety of corrosive environments [26-29]. The corrosion behavior of the API X-65 pipeline steel in 1.0 M H₂SO₄ solution was investigated using EIS method and the Nyquist plots obtained for this steel after its immersion in 1.0 M H₂SO₄ solution for (1) 10 min, (2) 60 min and (3) 24 h at room temperature are depicted in Fig. 4. The Nyquist plots represented in Fig. 4 were analyzed by best fitting to the equivalent circuit model

shown in Fig. 5 and the values of the symbols of this circuit are listed in Table 4. These parameters can be defined according to usual convention, as follows; R_s represents the solution resistance, R_p is the polarization resistance and can also be defined as the charge transfer resistance, and Q is the constant phase elements (CPEs).

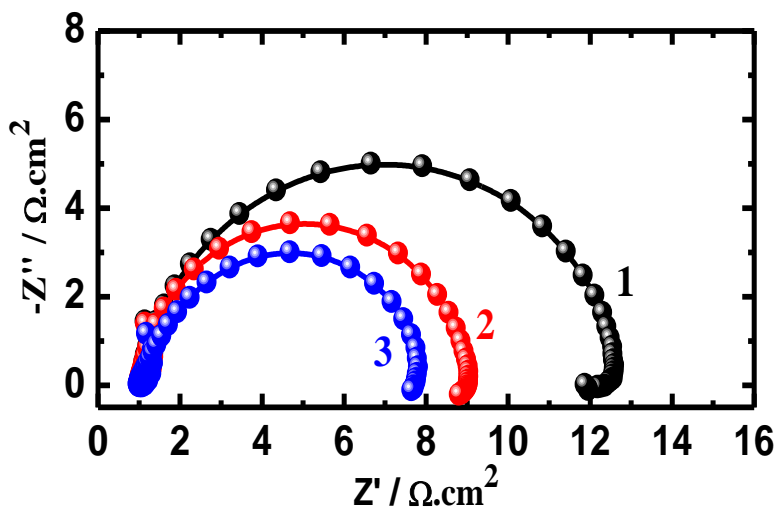


Figure 4. Typical Nyquist plots obtained for X-65 5L pipeline steel samples after (1) 10 min, (2) 60 min and (3) 24 h immersion in 1.0 M H_2SO_4 solutions at room temperature.

It is seen from Fig. 4 that only one depressed semicircle is shown and its diameter increases with increasing the immersion time from 10 min to 24 h. The deviation from ideal semicircle is generally attributed to the frequency dispersion as well as to the inhomogeneities of the surface and mass transport resistant [30,31]. The capacitance loop intersects the real axis at higher and lower frequencies. At high frequency end the intercept corresponds to R_s and at lower frequency end corresponds to the sum of R_s and R_p . It is also seen from Table 4 and Fig. 5 that the values of R_s and R_p decreased, while the value of the Q (CPEs) increased with increasing immersion time. According to Macdonald et al. [32], the Q with their n values less than one, represent impure double layer capacitance to reduce the effects due to surface irregularities of the X-65 pipeline steel.

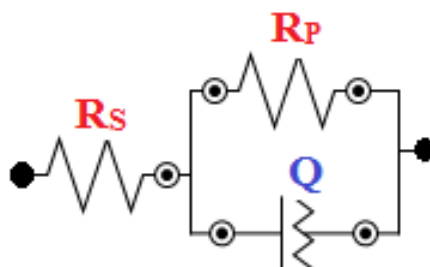


Figure 5. The equivalent circuit model used to fit the EIS experimental data shown in Fig. 4; the symbols of the circuit are defined in text and their values are listed in Table 4.

Table 4. EIS parameters of the API pipeline X-65 steel after its immersion in 1.0 M H₂SO₄ for 10 min, 60 min, and 24 h, respectively.

Time	EIS parameters			
	R _s / Ω cm ²	CPE / μMho	N	R _p / Ω cm ²
10 min	1.10	128	0.905	11.8
60 min	1.06	599	0.946	7.95
24 h	1.00	5600	0.887	6.22

In order to confirm the EIS Nyquist spectra for the steel in the sulfuric acid solution, we presented the Bode impedance plots. Fig. 6 shows the Bode impedance plots that obtained for the API X-65 5L pipeline steel after (1) 10 min, (2) 60 min and (3) 24 h immersion in 1.0 M H₂SO₄ solutions at room temperature. It is clearly seen from Fig. 2 that there is only one time constant, which is corresponding to one depressed semicircle that obtained in the case of Nyquist plots. It is also seen that the increase of immersion time decreased the absolute impedance values across the whole range of applied frequency.

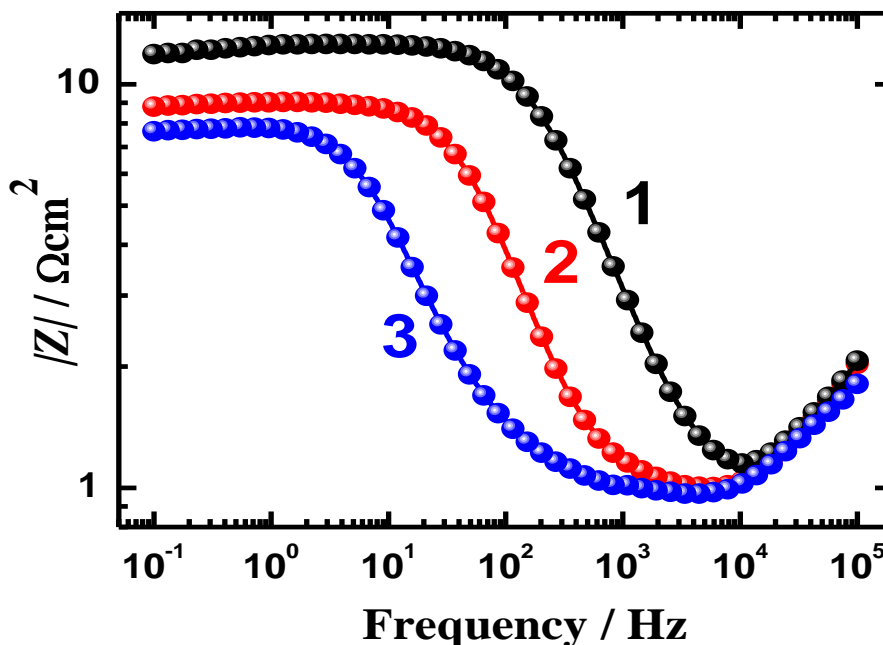


Figure 6. Bode impedance plots obtained for the API X-65 5L pipeline steel after (1) 10 min, (2) 60 min and (3) 24 h immersion in 1.0 M H₂SO₄ solutions at room temperature.

The effect of increasing temperature on the corrosion of the API X-65 steel in 1.0 M H₂SO₄ solutions, the EIS measurements were also carried out. Fig. 7 shows typical Nyquist plots obtained for

the API X-65 steel in 1.0 M H₂SO₄ solutions at (1) 20 °C, (2) 30 °C, (3) 40 °C, (4) 50 °C and (5) 60 °C, respectively. The data presented in Fig. 7 were best fitted to the equivalent circuit shown in Fig. 5 and the values of the parameters of the circuit are listed in Table 4. In order to confirm the results obtained from the EIS Nyquist spectra, we plotted the Bode impedance curves as shown in Fig. 8. The results of the Bode plots indicated that the increase of temperature decreases the impedance of the interface overall the applied frequency range, which reveals that increasing the temperature of the sulfuric acid decreases the resistance of the API X-65 steel.

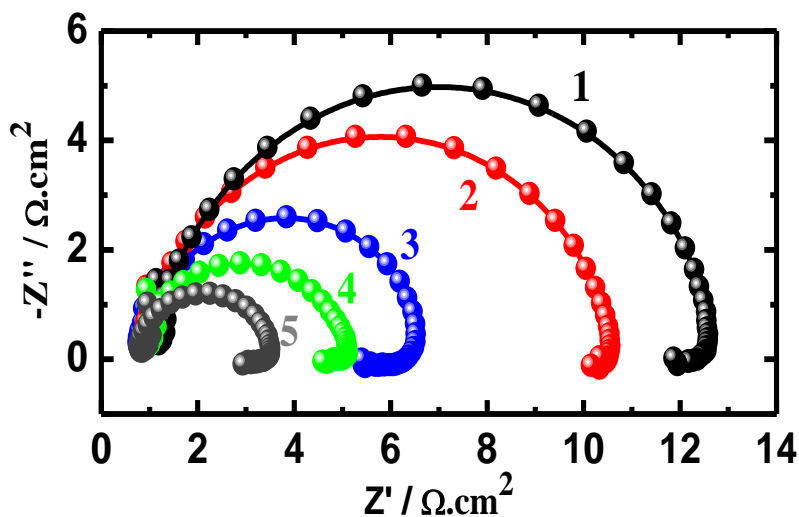


Figure 7. Nyquist plots obtained for the API X-65 steel after 30 min immersion in 1.0 M H₂SO₄ solutions at (1) 20 °C, (2) 30 °C, (3) 40 °C, (4) 50 °C and (5) 60 °C, respectively.

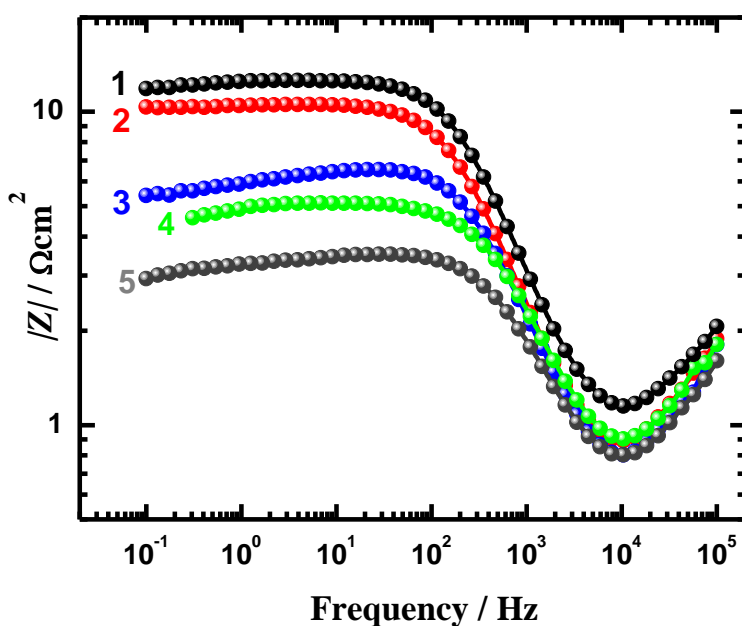


Figure 8. Bode impedance plots obtained for the API X-65 steel after 30 min immersion in 1.0 M H₂SO₄ solutions at (1) 20 °C, (2) 30 °C, (3) 40 °C, (4) 50 °C and (5) 60 °C, respectively.

It is seen from Fig. 7 that the shape of Nyquist plots is similar to that obtained at room temperature, Fig. 4 and the diameter of the semicircle decreases as solution temperature increases. It is also seen from Table 4 that the increase of temperature from 20 °C to 60 °C remarkably decreased the values of the resistances, R_s and R_p . This effect was also found to increase the value of the obtained CPEs. Moreover, the Bode impedance plots shown in Fig. 8 indicated that the impedance of the interface of the X-65 steel decreases with increasing temperature. The EIS data together confirm that the increase of the sulfuric acid temperature increases the corrosion of the API X-65 steel.

Table 5. EIS parameters obtained for the API X-65 pipeline steel after 30 min immersion in 1.0 M H_2SO_4 solutions at different temperatures.

Temperature	Impedance parameters			
	$R_s / \Omega \text{ cm}^2$	CPE / μMho	n	$R_p / \Omega \text{ cm}^2$
20 °C	1.0	128	0.905	11.80
30 °C	0.84	157	0.883	9.88
40 °C	0.73	198	0.916	6.00
50 °C	0.71	202	0.881	4.35
60 °C	0.68	209	0.905	2.88

4. DISCUSSION

The coarse grains, residual stresses due to shrinkage, their corresponding lattice strains, and the disordered crystals in the API X-65 steel all of which favor the formation of microcell corrosion in the sulfuric acid solution. This is because the sensitivity of X-65 steel towards corrosion has a great relation with its microstructure. Recent experimental research [33] showed that X-65 steel has a ferrite-pearlitic structure that affects its resistant to crack initiation in the near-neutral pH groundwater.

Increasing the immersion time from 10 min to 60 min and further to 24 h led to increasing corrosion of X-65 steel as confirmed by the polarization curves shown in Fig. 2. It has been reported [28,34] that the cathodic reaction for metals and alloys in sulfuric acid solutions is the hydrogen evolution as follows,



On the other hand, the anodic reaction is the dissolution of iron of the alloy, which consumes the electrons produced at the cathode according to the following reaction,



Increasing the immersion time increases the dissolution of the steel via the corrosion of iron under the continuous attack of sulfuric acid to the alloys surface, which does not allow the alloy to

form any oxide and/or corrosion products that can reduce the corrosion [28]. Increasing the applied potential in the less negative direction further facilitates the corrosion of steel as indicated by the increase of the anodic currents with potential and with the increase of immersion time. This was reflected on the increased values of j_{Corr} and the decreased values of R_p for the steel with time as listed in Table 2. This effect was also observed from EIS Nyquist plots shown in Fig. 4 and also the EIS plots for the impedance of the interface depicted in Fig. 6. Where, increasing the immersion time decreases the diameter of semicircle as well as the impedance of the interface for the API X-65 steel in 1.0 M H_2SO_4 solutions. Table 4 also confirmed that both solution and polarization resistances decrease, while the constant phase elements (Q, CPEs) increases with time. This supports the idea that the corrosion of the X-65 steel is controlled by a charge transfer process [34] that increases its rate with increasing the time.

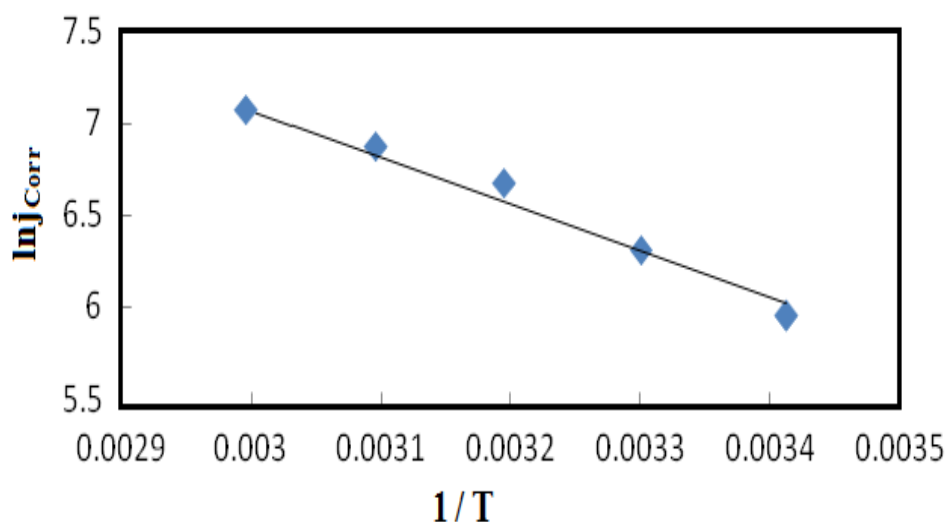


Figure 9. Arrhenius plots for the dissolution for the API X-65 steel in 1.0 M H_2SO_4 solutions.

The effect of increasing temperature on the corrosion of the API X-65 steel in 1.0 M H_2SO_4 solutions was investigated using polarization, EIS, Arrhenius, and activation energy measurements at different temperatures between 20 °C to 60 °C. The polarization data shown in Fig. 3 and the corrosion parameters listed in Table 3 indicated that the corrosion of the X-65 steel increases remarkably with the increase of temperature. The positive shift in the corrosion potential (E_{Corr}) indicates that the anodic process is more affected than the cathodic one [35]. The little change of β_a and β_c with solution temperature indicates that there is a little change in the mechanism of corrosion with temperature. The increase of the anodic and cathodic currents and the values of j_{Corr} and conjunctly the decrease of R_p confirm that the X65 steel suffers more corrosion with increasing temperature. The EIS plots shown in Fig. 7 and Fig. 8 and also the EIS parameters listed in Table 5 provided another confirmation on the effect of increasing temperature on the corrosion of the X65 steel in the tested sulfuric acid solution. This is because increasing temperature decreased both the diameter of the semicircle (Fig. 7) as well as the impedance of the interface (Fig. 8). This effect also decreased the values of R_s and R_p and

increased the values of the CPEs as can be seen from Table 5. The results of the EIS Nyquist and Bode plots agree with the obtained data by polarization measurements.

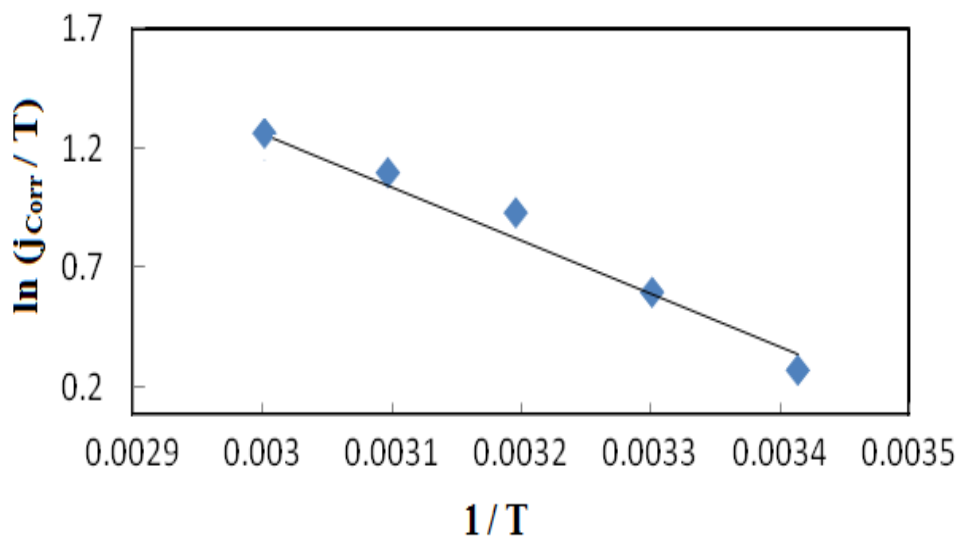


Figure 10. ln(corrosion rate/T) vs. 1/T for the API X-65 steel in 1.0 M H₂SO₄ solutions.

In order to confirm the effect of increasing the sulfuric acid temperature on the corrosion of the API X-65 pipeline steel, the activation energy (E_a) was calculated from the Arrhenius equation as follows [36],

$$\ln(j_{\text{Corr}}) = B - \left(\frac{E_a}{RT} \right) \tag{3}$$

Where, B is a constant that depends on the metal type and R is the universal gas constant. The plot of $\ln(j_{\text{Corr}})$ versus the reciprocal of absolute temperature (1/T) gives a straight line whose slope = - (E_a / R), from which the activation energy values for the corrosion process were calculated. The Arrhenius plots for the X-65 steel specimens are shown in Fig. 9. The enthalpy (ΔH) and entropy (ΔS) of activation were calculated from transition state theory according to the following equation [36];

$$j_{\text{Corr}} = \left(\frac{RT}{Nh} \right) \exp \frac{\Delta S}{R} \exp \frac{-\Delta H}{RT} \tag{4}$$

Here, h is Planck's constant and N is Avogadro's number. A plot of $\ln(j_{\text{Corr}}/T)$ versus 1/T gives a straight line with slope = $-\Delta H/R$ and intercept = $\ln(R/Nh) + \Delta S/R$. Fig. 10 shows the relationship between $\ln(j_{\text{Corr}}/T)$ and 1/T for the corrosion of the X-65 steel specimens in the 1.0 M sulphuric acid solutions. The activation parameters calculated are listed in Table 6.

Table 6. Activation energy parameters of corrosion reactions for X65 steel in 1.0 M H₂SO₄.

$E_a(\text{Kj/mol})$	$\Delta H (\text{Kj/mol})$	$\Delta S(\text{J/mol/K})$
21.08	18.49	-131.41

The activation energy values obtained for the X-65 steel specimens confirmed that the whole corrosion process is controlled by surface reaction, since the values of E_a for the corrosion process are greater than 20 kJ/mol [37]. Another confirmation was given by the negative values recorded of the entropy of activation, ΔH . This implies that the activated complex in the rate-determining step represents association rather than dissociation, indicating that a decrease in randomness takes place on going from reactants to the activated complex [38]. The results obtained from activation energy thus confirm the ones obtained by polarization and EIS that the increase of the temperature significantly activates the surface of the API X-65 pipeline steel and therefore increases its corrosion in the 1.0 M H_2SO_4 solution.

5. CONCLUSIONS

The effects of immersion time and temperature on the electrochemical corrosion behavior of API 5L grade X-65 steel in 1.0 M H_2SO_4 pickling solutions were reported. The study was carried out by using optical microscopy, potentiodynamic polarization, and EIS measurements. The polarization and EIS measurements indicated that increasing the immersion time increases the corrosion of the API 5L grade X-65 steel in 1.0 M H_2SO_4 solutions. This is because the increase of immersion time increases the values of anodic current, cathodic current and j_{Corr} , while decreases the surface (R_s) and polarization (R_p) resistances, which reflects on the increase of the corrosion rate with time. The increase of time of immersion also shifted the values of E_{Corr} towards the less negative direction. It has been also found that the increase of temperature of the solution highly increases the dissolution of the steel through increasing the reactivity of its surface. Where, the increase of temperature led to increasing the corrosion rate and decreasing the corrosion resistance of the steel in the tested acid solution. This was further confirmed by the calculated values of activation energy, E_a , which were greater than 20 kJ/mol at all tested temperatures indicating that the corrosion process of the X-65 pipeline steel was controlled by its surface reactions.

ACKNOWLEDGEMENTS

The authors would like to extend their sincere appreciation to the Deanship of Scientific Research at King Saud University for its funding of this research through the Research Group Project No. RGP-VPP-160.

References

1. A. Yakubtsov, P. Poruks, J. D. Boyd, *Mater. Sci. Eng. A*, 480 (2008) 109.
2. M. C. Zhao, K. Yang, Y. Y. Shan, *Mater. Lett.* 57 (2003) 1496.
3. E.-S. M. Sherif, A. A. Almajid, *J. Chem.*, 2014 (2014) Article ID 753041, 7 pages.
4. H. Iken, R. Basseguy, A. Guenbour, A. Ben Bachir, *Electrochimica Acta*, 52 (2007) 2580.
5. T. Poornima, J. Nayak, A. N. Shetty, *Portugaliae Electrochimica Acta*, 28 (2010) 173.
6. A. Guenbour, M. A. Hajji, E. M. Jallouli, A. Ben Bachir, *Appl. Surf. Sci.*, 253 (2006) 2362.
7. A. Bellaouchou, B. Kabkab, A. Guenbour, A. Ben Bachir, *Prog. Org. Coat.*, 41 (2001) 127.
8. F. Bentiss, M. Traisnel, M. Lagrenee, *Corros. Sci.*, 42 (2000) 127.

9. S. Ghareba, S. Omanovic, *Corros. Sci.*, 52 (2010) 2104.
10. A. A. Al-Amiery, A. A. H. Kadhum, A. Kadhum, A. B. Mohamad, C. K. How, S. Junaedi, *Materials*, 7 (2014) 787.
11. A. Hernández-Espejel, M. A. Domínguez-Crespo, R. Cabrera-Sierra, C. Rodríguez-Meneses, E. M. Arce-Estrada, *Corros. Sci.*, 52 (2010) 2258.
12. M. A. Hegazy, H. M. Ahmed, A. S. El-Tabei, *Corros. Sci.*, 53 (2011) 671.
13. M. A. Migahed, *Prog. Org. Coat.*, 54 (2005) 91.
14. S. Nešić, *Corros. Sci.*, 49 (2007) 4308.
15. J. W. Graves, E. H. Sullivan, *Mater. Prot.*, 5 (1996) 33.
16. N. Muthukumar, S. Maruthamuthu, N. Palaniswamy, *Colloids Surf. B: Biointerf.*, 53 (2006) 260.
17. A. Rajasekar, T. Ganesh Babu, S. Karutha Pandian, S. Maruthamuthu, N. Palaniswamy, A. Rajendran, *Corros. Sci.*, 49 (2007) 2694.
18. D. Hardie, E. A. Charles, A. H. Lopez, *Corros. Sci.*, 48 (2006) 4378.
19. Y. F. Cheng, *Int. J. Hyd. Energy*, 32 (2007) 1269.
20. C. T. Kwok, S. L. Fong, F. T. Cheng, H. C. Man, *J. Mater. Proc. Technol.*, 176 (2006) 168.
21. F.Y. Ma, W.H. Wang, *Mater. Sci. Eng. A*, 430 (2006) 1.
22. J. Y. Lee, S. M. Lee, *Surf. Coatings Technol.*, 28 (1986) 301.
23. G. M. Pressouyre, I. A. Bernstein, *Metallurgical Transactions A*, 10 (1978) 1571.
24. E. Villalba, A. Atrens, *Engineering Failure Analysis*, 15 (2008) 617.
25. E.-S. M. Sherif, H. R. Ammar, A. K. Khalil, *Appl. Surf. Sci.*, 301 (2014) 142.
26. E.-S. M. Sherif, A. A. Almajid, A. K. Khalil, H. Junaedi, F. H. Latief, *Int. J. Electrochem. Sci.*, 8 (2013) 9360.
27. K. Darowicki, S. Krakowiak, P. Ślepski, *Electrochimica Acta*, 49 (2004) 2909.
28. E.-S. M. Sherif, *Appl. Surf. Sci.*, 292 (2014) 190.
29. E.-S. M. Sherif, *Ind. Eng. Chem. Res.* 52 (2013) 14507.
30. H. H. Hassan, E. Abdelghani, M. A. Amin, *Electrochimica Acta*, 52 (2007) 6359.
31. P. Bommersbach, C. Alemany-Dumont, J. P. Millet, B. Normand, *Electrochimica Acta*, 51 (2005) 1076.
32. W. B. Johnson, J. R. Macdonald, "Theory in impedance Spectroscopy, experiments and applications," John Wiley & Sons, New York, 2005.
33. B. T. Lu, J. L. Luo *Corrosion*, 62 (2006) 723.
34. E.-S. M. Sherif, *Int. J. Electrochem. Sci.*, 6 (2011) 2284.
35. A. El-Sayed, *J. Appl. Electrochem.*, 27 (1997) 193.
36. F. Bentiss, M. Lebrini, M. Lagrenée, *Corros. Sci.*, 47 (2005) 2915.
37. K. K. El-Neami, A. K. Mohamed, I. M. Kenawy, A. S. Fouda, *Monatshefte für Chemie / Chemical Monthly*, 126 (1995) 369.
38. S. S. Abd El-Rehim, M. A. M. Ibrahim, K. F. Khaled, *J. Appl. Electrochem.*, 29 (1999) 593.